Three-neutron bound and continuum states

Souichi Ishikawa ●[*]

Science Research Center, Hosei University, 2-17-1 Fujimi, Chiyoda, Tokyo 102-8160, Japan

The three-neutron ($3n$) system is studied by numerical calculations with the Faddeev three-body formalism for a realistic nucleon-nucleon (NN) potential. A response function for the transition from ^{3}H to $3n$ continuum states by an isospin excitation operator is calculated, from which no evidence of $3n$ resonance state is found. Different methods to extrapolate the $3n$ energy from bound state energies with an extra attractive effect to the NN potential are examined. While extrapolations with attractive effects by enhanced NN potentials or three-body potentials result in the nonexistence of $3n$ resonance states, one by external trapping potentials leads to a positive $3n$ energy, which may be considered as a resonance state. It is found that this contradiction is due to a general defect of the trapping method.

I. INTRODUCTION

Studies of few-neutron systems are expected to enrich our knowledge of the interaction among neutrons, which is essential to microscopic understanding of neuron-rich nuclei and neutron matter. For a neutron-neutron (nn) system there exists a virtual state, which results a peak in energy spectra of reactions leaving two neutrons in the final state, such as the $\pi^- d \rightarrow nn\gamma$ reaction, and gives us information of the ${}^1S_0$ scattering length (see, e.g., Ref. [1]). There has been no conclusive evidence for the existing of bound or resonance state in $3n$ (e.g., Ref. [2]) and four-neutron ($4n$) systems, besides a few experimental suggestions for a resonant $4n$ state [3,4].

Recently, the existence of $3n$ as well as $4n$ resonance states was indicated by quantum Monte Carlo calculations [5] and no-core Gamow shell model calculations [6]. However, these calculations contradict previous calculations [7–10] (see also Refs. [11–13]) by the Faddeev-type method [14], which showed that complex energy eigenvalues of the Hamiltonians of the systems are too far from the real energy axis to give any effect as a resonance. The aim of this paper is to clarify a reason of this discrepancy by performing Faddeev $3n$ calculations for continuum and bound states.

In Refs. [7,8], the Faddeev equations [14] were solved in combination with the complex scaling method, from which one can obtain a complex energy eigenvalue of the system, $E_r - i\frac{\Gamma}{2}$ with E_r being the resonance energy and Γ the width. On the other hand, in Ref. [10], the transition amplitude for $3n \rightarrow 3n$ scattering was calculated at positive real energies, from which the pole position of the amplitude in the complex energy plane is evaluated.

Since the $3n \rightarrow 3n$ scattering cannot be performed as a laboratory experiment, in the present paper I will study one of possible realization of $3n$ continuum systems, namely the charge exchange reaction ^{3}H(n, p)$3n$. Actually, there have been some experimental works for its mirror reaction, ^{3}He(p, n)$3p$ [15,16]. In Ref. [17], this reaction was studied in a plane wave impulse approximation (PWIA), in which response functions of the transition from ^{3}He to the three-proton ($3p$) state by spin-isospin transition operators were calculated in the Faddeev three-body formalism.

The response function is written as the imaginary part of a matrix element of the Green's function for the $3n$ Hamiltonian [see Eq. (7) below]. A complex eigenvalue of the Hamiltonian corresponds to the pole of the Green's function in the complex energy plane. If the pole is close to positive energy axis in the fourth quadrant so that the response function has a peak as a function of the (real) energy, one may recognize that a resonance state exists.

In the above mentioned calculations, to realize a bound state or a resonance state artificially, an additional attractive effect is given on the original Hamiltonian either by enhancing the nn interaction [7,8,10], by introducing a three-body force [8], or by introducing an external potential that confines the neutrons in a trap [5,6]. Energies are calculated with modifying the strength of the attractive effect, from which the energy for the original Hamiltonian is extracted.

In Sec. II, three-body calculations of the response function will be described. In Sec. III, results of the response function as well as the $3n$ binding energy for modified $3n$ Hamiltonians are presented, and the extrapolation methods will be examined. In Sec. IV, results of $3n$ calculations will be interpreted in a simple two-body system. A summary will be given in Sec. V.

II. RESPONSE FUNCTION

In this paper, I will study a response function corresponding to ^{3}H bound state to $3n$ continuum state by an isospin excitation operator:

$$\hat{O}(Q) = \sum_{i=1}^{3} e^{iQ\hat{z}\cdot r_i} t_i^{(-)}, \tag{1}$$

* ishikawa@hosei.ac.jp

where Q is the momentum transfer, $t_i^{(-)}$ an isospin operator that transforms the proton i in ^{3}H to neutron i in the final $3n$ state, and $\mathbf{r}_i$ the coordinate vector in the three-nucleon center-of-mass (c.m.) system of the particle i. This is one of three transition operators to used in PWIA analysis of the ^{3}H$(n, p)3n$ reaction.

First, I introduce the $3n$ Hamiltonian in the c.m. system,

$$H_{3n} = H_0 + \sum_i V_i^{(2B)} + \sum_i V_i^{(3B)}, \qquad (2)$$

where H_0 is the three-body kinetic energy operator, $V_i^{(2B)}$ is an two-body potential between particles j and k, and $V_i^{(3B)}$ is a three-body potential (3BP) that is symmetric with respect to particles j and k.

Let $|\Psi^{(\pm)}(q, p; J^\pi)\rangle$ be an eigenstate of the $3n$ Hamiltonian $H_{3n}(J^\pi)$ for the total angular momentum J and parity π state associated with an asymptotic $3n$ state, in which the relative momentum between two neutrons is q and the momentum of the third neutron with respect to c.m. of the neutron pair is p. The superscript $(\pm)$ expresses the outgoing $(+)$ or incoming $(-)$ boundary condition.

The eigenvalue problems is written as

$$H_{3n}(J^\pi)|\Psi^{(\pm)}(q, p; J^\pi)\rangle = E(q, p)|\Psi^{(\pm)}(q, p; J^\pi)\rangle, \qquad (3)$$

with

$$E(q, p) = \frac{q^2}{m} + \frac{3p^2}{4m}, \qquad (4)$$

where m is the mass of the neutron.

A response function corresponding to the transition from the ^{3}H bound state, $|\Psi_t\rangle$, to $3n$-continuum states with energy E by an operator $\hat{O}(Q)$ is written as

$$R(E, Q; J^\pi) = \int dq\, dp |T(q, p; Q, J^\pi)|^2 \delta(E - E(q, p)), \qquad (5)$$

where the transition amplitude is defined by

$$T(q, p; Q, J^\pi) = \langle \Psi^{(-)}(q, p; J^\pi)|\hat{O}(Q)|\Psi_t\rangle. \qquad (6)$$

Using the completeness of the $3n$ states, one finds

$$\begin{aligned} R(E, Q; J^\pi) &= \langle \Psi_t|\hat{O}^\dagger(Q)\delta(E - H_{3n}(J^\pi))\hat{O}(Q)|\Psi_t\rangle \\ &= -\frac{1}{\pi}\text{Im}\langle \Psi_t|\hat{O}^\dagger(Q)\frac{1}{E + i\epsilon - H_{3n}(J^\pi)}\hat{O}(Q)|\Psi_t\rangle. \end{aligned} \qquad (7)$$

Here, I introduce a wave function $|\Xi(Q, J^\pi)\rangle$ describing the disintegration process,

$$|\Xi(Q, J^\pi)\rangle = \frac{1}{E + i\epsilon - H_{3n}(J^\pi)}\hat{O}(Q)|\Psi_t\rangle. \qquad (8)$$

Adapting the Faddeev theory to solve Eq. (8), a three-body wave function $|\Xi\rangle$ is decomposed into three (Faddeev) components:

$$|\Xi\rangle = |\Phi^{(1)}\rangle + |\Phi^{(2)}\rangle + |\Phi^{(3)}\rangle, \qquad (9)$$

where I drop the arguments Q and J^π for simplicity. Corresponding to this decomposition, the operator $\hat{O}$ is decomposed into three components:

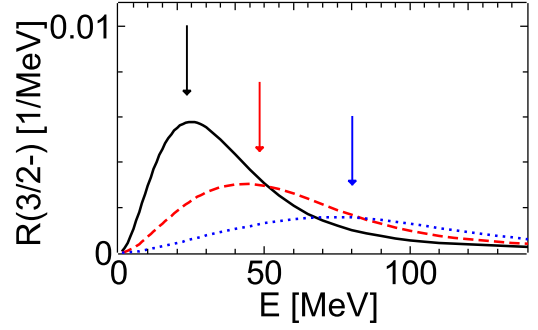$$\hat{O} = \hat{O}_1 + \hat{O}_2 + \hat{O}_3, \qquad (10)$$

FIG. 1. Energy dependence of the response function $R(E, Q; \frac{3}{2}^-)$ for $Q = 300$ MeV/c (black solid curve), $Q = 400$ MeV/c (red dashed curve), and $Q = 500$ MeV/c (blue dotted curve) calculated with AV18. The black, red, and blue arrows indicate the energies given by Eq. (13) for $Q = 300$, 400, and 500 MeV/c, respectively.

with the condition that $\hat{O}_i$ is symmetric with respect to the exchange of j and k. Then Faddeev equations read

$$\begin{aligned} |\Phi^{(1)}\rangle &= G_1(E)\hat{O}_1|\Psi_t\rangle + G_1(E)V_1^{(2B)}|\Phi^{(2)} + \Phi^{(3)}\rangle \\ &\quad + G_1(E)V_1^{(3B)}|\Phi^{(1)} + \Phi^{(2)} + \Phi^{(3)}\rangle \\ &\quad \text{(and cyclic permutations)}, \end{aligned} \qquad (11)$$

where the operator $G_i(E)$ is a channel Green's function defined as

$$G_i(E) \equiv \frac{1}{E + i\varepsilon - H_0 - V_i^{(2B)}}. \qquad (12)$$

The Faddeev equations, Eq. (11), are solved as integral equations in coordinate space, whose formal and technical details are essentially same as those used for the nucleon-deuteron scattering [18,19] and three-alpha-particle [20] problems. The amplitude, Eq. (6), is calculated from the solution.

In the present work, I will use the Argonne v_{18} model (AV18) [21] for the NN potential, taking partial waves with angular momenta $j \leqslant 4$. The ^{3}H wave function for the initial state is calculated with AV18 and the Brazil 2π-exchange type three-nucleon potential, BR-$\mathcal{O}(q^4)$, in Ref. [22].

III. 3n CALCULATIONS

I will consider the transition from the ^{3}H ground state to $3n(\frac{3}{2}^-)$ continuum state. This final state was reported to be the most preferable in a sense that the modification of the original nuclear interaction to produce a resonance state could be minimal [7,8], and is considered to be the state found in Ref. [5].

Figure 1 displays the response functions $R(E, Q; \frac{3}{2}^-)$ for $Q = 300$, 400, and 500 MeV/c calculated with AV18 as functions of E. The figure shows that the response functions have a peak at the energy, which varies with Q. The vertical arrows indicate the energies calculated by

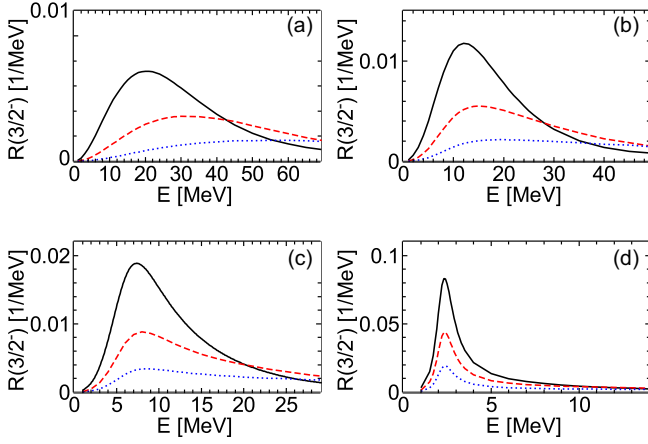$$E = \frac{Q^2}{2m} - B(^3\text{H}) - \frac{Q^2}{6m}, \qquad (13)$$

FIG. 2. Energy dependence of the response function $R(E, Q; \frac{3}{2}^-)$ calculated by $^3P_2$-$^3F_2$ modified AV18 with (a) $\alpha = -1.0$, (b) $\alpha = -2.0$, (c) $\alpha = -2.4$, and (d) $\alpha = -2.8$. In each figure, black solid, red dashed, and blue dotted curves denote for $Q = 300$, 400, and 500 MeV/c, respectively.

FIG. 3. Calculated 3n energies for AV18 as functions of the factor α. Black circles are calculated values of the 3n binding energy. Black dashed curves are obtained by fitting the 3n binding energy. Green triangles are the peak energies of the response functions. Red squares are extracted values of E_r, with error bars being $\pm\frac{1}{2}\Gamma$ from the response functions using Eq. (14).

where $B(^3\text{H})$ is the ^{3}H binding energy. This value means that the momentum Q is absorbed by one neutron, which leads to a quasifree process. The peak energy of the response function for each of Q almost coincides with the one given by Eq. (13), which shows that the peaks of $R(E, Q)$ are not due to a resonance pole.

In the following, I will examine three extrapolation procedures with giving additional attractions to the 3n Hamiltonian: (i) by multiplying a factor to the nn potential to enhance an attractive contribution; (ii) by introducing a 3BP; and (iii) by introducing additional potential that traps neutrons around their center of mass.

(i) The factor multiplied to the nn potential will be denoted by $(1 - \alpha)$. Since a rather small value of α, e.g., -0.080 for AV18, makes the $nn(^1S_0)$ system bind [8], the factor will be multiplied only to the $^3P_2$-$^3F_2$ partial wave component of the nn potential, which is known to be attractive. In this notation, a negative value of α gives an attractive effect. In fact, an $nn(^3P_2$-$^3F_2)$ bound state exists for $\alpha < -3.39$, and a $3n(\frac{3}{2}^-)$ bound state exists for $\alpha < -2.98$. These values agree with those obtained in Ref. [8].

The response functions for $Q = 300$, 400, and 500 MeV/c calculated by $^3P_2$-$^3F_2$ modified AV18 with $\alpha = -1.0$, -2.0, -2.4, and -2.8 are displayed in Fig. 2. As the attractive effect becomes larger, the Q dependence of the peak energy does weaker. For $\alpha < -2.0$, the peak energies are almost Q independent, and are plotted as green triangles in Fig. 3 as a function of α.

Since the peak energy may not necessarily be the resonance energy, I will test to fit the response function by the following expression:

$$R(E) = \frac{b(E - E_r) + c\Gamma}{(E - E_r)^2 + \Gamma^2/4} + a_0 + a_1(E - E_r) + a_2(E - E_r)^2, \quad (14)$$

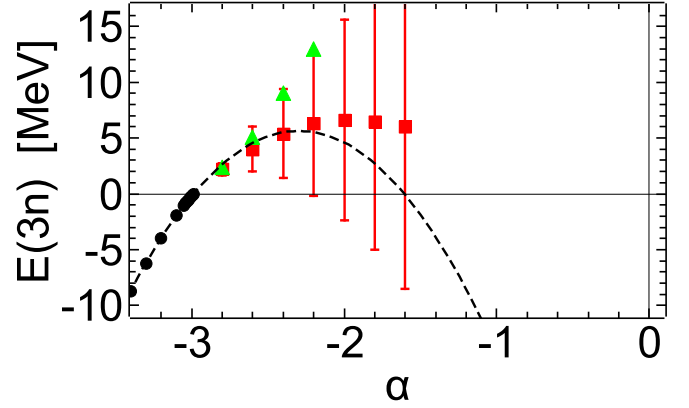which has a form of the Lorentz function taking into account some asymmetric effects. The parameters E_r, Γ, a_n

($n = 0, 1, 2$), b, and c are obtained from the response function for $E \leqslant 30$ MeV. Here the complex value $E_r - i\frac{\Gamma}{2}$ could be a pole energy of the Green's function in the complex plane. Extracted values of E_r and Γ are Q independent for $-2.7 \leqslant \alpha \leqslant -1.6$. In Fig. 3, extracted values of E_r are plotted as red squares with error bars being $\pm\frac{1}{2}\Gamma$. As the attractive effect is reduced, E_r increases and stays at about 6.5 MeV with increasing width, which reaches about $\Gamma = 30$ MeV at $\alpha = -1.6$. Numerical errors of E_r and Γ in the extraction are as small as 10^{-3} MeV for $\alpha = -2.7$, and increase as the magnitude of α becomes small: about 0.4 MeV for $\alpha = -1.6$. Extracted values of E_r and Γ are Q dependent for $\alpha > -1.6$, which indicates that the complex value $E_r - i\frac{\Gamma}{2}$ is away from the real energy axis. These tendencies in the obtained values of (E_r, Γ) are similar to those from the $3n \rightarrow 3n$ amplitude with $^3P_2$-$^3F_2$ modified nn potentials in Ref. [10].

Calculated values of the $3n(\frac{3}{2}^-)$ binding energy for $\alpha < -3.0$ are plotted as black circles in Fig. 3. As shown in the figure, both of the peak energies and the extracted E_r appear to be smoothly connected to the binding energies. An extrapolation is performed by fitting the 3n binding energies with a quadratic polynomial of α, which is chosen just for its simplicity. The result is plotted as black dashed curve in the figure, which approximately follows the extracted E_r rather than the peak energy.

(ii) The introduction of an attractive 3BP is another way to bring an extra attractive effect. In Ref. [17], the response functions for spin-isospin transitions from ^{3}He ground state to $3p$ continuum state are calculated, introducing a 3BP to produce a $3p$ resonance. Here, I will apply the same functional form of 3BP, which was taken from Ref. [23]:

$$V_i^{(3B)} = \frac{1}{3} \sum_{n=1}^{2} W_n e^{-(r_{ij}^2 + r_{jk}^2 + r_{ki}^2)/b_n^2}, \quad (15)$$

where r_{ij} is the distance between the ith and jth neutrons. Note that this form of $V_i^{(3B)}$ is totally symmetric under the
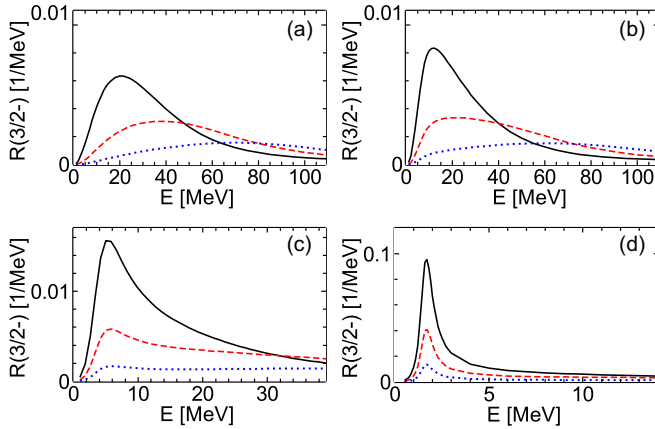
FIG. 4. Energy dependence of the response function $R(E, Q; \frac{3}{2}^-)$ calculated with AV18 + 3BP for (a) $W_1 = -10$ MeV, (b) $W_1 = -30$ MeV, (c) $W_1 = -50$ MeV, and (d) $W_1 = -70$ MeV. In each figure, black solid, red dashed, and blue dotted curves denote $R(E, Q; \frac{3}{2}^-)$ for $Q = 300$, 400, and 500 MeV/c, respectively.

particle exchange and the total 3BP is obtained by summing up all cyclic permutations of Eq. (15), and the factor 1/3 arises because of that. The range parameters and the strength parameters of the shorter range term are the same ones as used in Refs. [23,24]: $b_1 = 4.0$ fm, $b_2 = 0.75$ fm, and $W_2 = 35.0$ MeV.

When the 3BP is applied to $3n(\frac{3}{2}^-)$ state with AV18, there is at least one 3n bound state for the attractive strength $W_1 < -80$ MeV. The value $W_1 = -80$ MeV contrasts with $W_1 = -2.55$ MeV that is determined to reproduce ^{3}H binding energy [17]. Also, it is noted that the required value of the strength parameter W_1 for the $4n(0^+)$ state to bind, as the lower bound of the experimental value [4], is -36.14 MeV [23].

Figure 4 shows the response functions for $Q = 300$, 400, and 500 MeV/c, calculated with AV18 plus 3BP of the strength parameter $W_1 = -10$, -30, -50, and -70 MeV. The dependence of the peak energy on Q becomes weak as the magnitude of W_1 increases. For $-80 < W_1 < -50$ MeV, the peak energies are almost Q independent, and are plotted as green triangles in Fig. 5.

Extracted values of E_r and Γ from the response functions using Eq. (14) are plotted in the form of $E_r \pm \frac{1}{2}\Gamma$ for $-80 < W_1 < -20$ MeV, where the values are Q independent. As the attractive effect is reduced, E_r increases and then decreases, having a maximum value of about 4 MeV and a width of about $\Gamma = 8$ MeV at $W_1 = -40$ MeV. Numerical errors of E_r and Γ in the extraction are about 10^{-4} MeV for $W_1 = -75$ MeV, and increase as the magnitude of the 3BP decreases: 0.1 MeV for $W_1 = -20$ MeV.

The calculated values of the 3n binding energy are plotted as black circles in Fig. 5, and a quadratic fit to these energies is shown as the black dashed curve. It is interesting to see that the fitted curve, in spite of its simple quadratic form, almost follows the extracted vales of E_r using Eq. (14).

The variations of (E_r, Γ) with respect to the parameters to modify the attractive effect in the cases (i) and (ii) are very similar to the pole trajectory obtained in the previous Faddeev
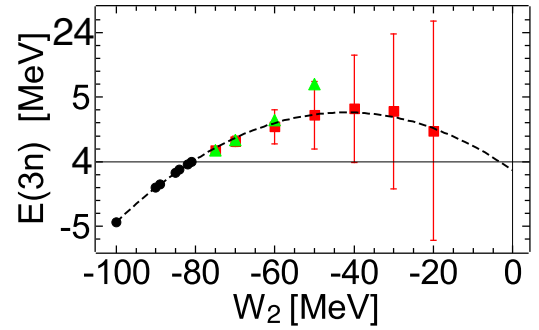

FIG. 5. Calculated 3n energies as functions of the 3BP strength parameter W_1. Black circles are calculated values of the 3n binding energy, and the black dashed curve is obtained by fitting the 3n binding. Green triangles are the peak energies of the response functions, and red squares are extracted values of E_r with error bars being $\pm\frac{1}{2}\Gamma$ from the response functions using Eq. (14).

calculations [8,10]. In both cases, the quadratic fitting of the 3n binding energy leads to a conclusion that there is no pole in the complex energy plane close to the real axis.

(iii) Next, I will examine the extrapolation using a trapping potential. As in Refs. [5,6], I use a potential of Woods-Saxon form with a radius R_{WS} and a diffuseness parameter $a_{WS} = 0.65$ fm,

$$W(r_i) = W_{WS} \frac{1}{1 + e^{(r_i - R_{WS})/a_{WS}}}, \qquad (16)$$

where r_i is the distance of ith neutron from the c.m. of the 3n system.

For the 3n bound state problem with the one-body potential $W(r_i)$, Faddeev calculations are performed in a way that the potential $W(r_1)$ is treated as same as the three-body potential $V_1^{(3B)}$ in Eq. (11). This treatment works well thanks to the limited range of wave functions for the bound state problem.

Calculated 3n binding energies for some values of R_{WS} are plotted in Fig. 6 as functions of the potential strength parameter W_{WS}. The curves are obtained by fitting the calculated energies with a quadratic polynomial of W_{WS}, and are extrapolated to $W_{WS} = 0$ MeV. Extrapolated 3n energies with
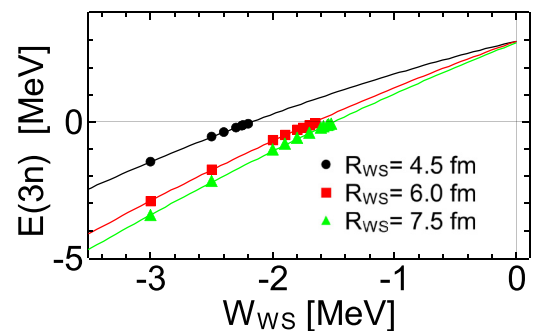

FIG. 6. Calculated 3n binding energies for AV18 as functions of the strength of the trapping potential W_{WS}. Black circles, red squares, and green triangles are calculated for the range parameter values $R_{WS} = 4.5$, 6, and 7.5 fm. Curves are obtained by fitting the points with a quadratic polynomial of W_{WS}.
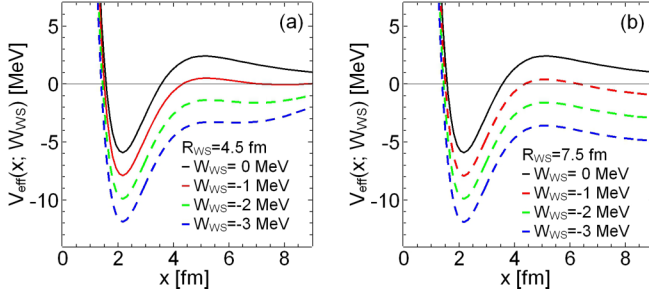
FIG. 7. The effective potentials for (a) $R_{WS} = 4.5$ fm and (b) $R_{WS} = 7.5$ fm. Black curves are for $W_{WS} = 0$ MeV, red curves for $W_{WS} = -1$ MeV, green curves for $W_{WS} = -2$ MeV, and blue curves for $W_{WS} = -3$ MeV. The meaning of solid and dashed curves is explained in the text.

FIG. 8. W_{WS} dependence of the energy of $2n$ p-wave state by the effective potential, Eq. (17), with $v_G = -50$ MeV. Black circles, red squares, and green triangles denote calculations by the trapping potentials with $R_{WS} = 4.5$ fm, 6.0 fm, and 7.5 fm. Curves are obtained by fitting the binding energies.

different R_{WS} values almost coincide with about 3 MeV. This may be the same result with one of Refs. [5,6], which suggests the existence of $3n$ resonance.

On the other hand, the results of the extrapolation methods (i) and (ii) demonstrate that the extrapolated $3n$ complex energy for the AV18 potential has a large negative imaginary part, and the real part of the energy may be negative, which indicates the nonexistence of $3n$ resonance.

These contradictory results throw some doubt on the reliability of the extrapolation method by a trapping potential. In the next section, a possible reason for this will be discussed.

IV. $2n$ SYSTEMS WITH GAUSSIAN POTENTIAL

Having in mind that a naive picture of $3n(\frac{3}{2}^-)$ state is a two-body system of the spin-singlet nn pair (dineutron) and the neutron in a P-wave ($L = 1$) state, I will apply the extrapolation method (iii) in the previous section to a two-body (two-neutron) P-wave system. In general, a P-wave resonance state may occur because of an attractive potential pocket within an exterior barrier caused by the centrifugal potential. Here, I define an effective potential $V_{eff}(x; W_{WS})$ as the sum of an attractive Gaussian potential, the P-wave centrifugal potential, and the trapping potential, Eq. (16):

$$V_{eff}(x; W_{WS}) = v_G \exp(-(x/r_G)^2) + \frac{\hbar^2 L(L+1)}{mx^2}$$
$$+ \sum_{i=1,2} W(r_i), \quad (17)$$

where x is the distance between two particles. In this study, I take the parameters of the Gaussian potentials as $r_G = 2.5$ fm and $v_G = -50$ MeV. The calculated P-wave scattering phase shift for this Gaussian potential takes a maximum of about $70°$ starting from $0°$ at zero energy, which means that the system does not have a resonance state.

The effective potentials $V_{eff}(x; W_{WS})$ for W_{WS} between -3 and 0 MeV taking the range parameter values of $R_{WS} = 4.5$ fm and $R_{WS} = 7.5$ fm are displayed in Fig. 7. In the figure, the solid curves indicate the potentials for which no bound state exists, and dashed curves indicate those for which a bound state exists.
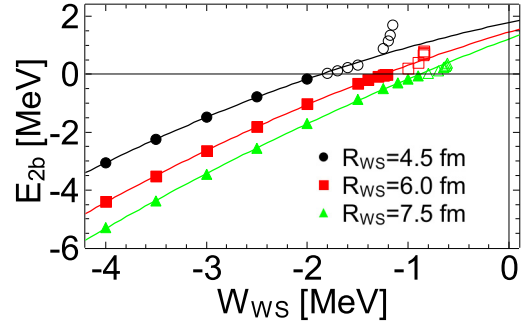
As the attractive effect becomes larger, the potential pocket spreads rapidly with vanishing barrier because the range of the trapping potential is longer than that of the Gaussian potential. In other words, as the attractive effect is reduced, the barrier appears at positive energy, which may cause an extra repulsive effect that does not exist for the bound states.

This extra repulsive effect is demonstrated in Fig. 8, which shows W_{WS} dependence of calculated values of the two-body energy for $R_{WS} = 4.5$ fm, 6.0 fm, and 7.5 fm. The dependence of the energy on W_{WS} in the bound state region is described by a quadratic polynomial, and leads to a positive energy at $W_{WS} = 0$ MeV. However, soon after getting into the continuum region, the dependence is quite different from that in the bound state region and the energy increases more than expected from the fitting, which indicates that the attractive effect becomes weak rapidly. Because of the rise in the continuum region, the extrapolation is no longer reliable.

V. SUMMARY

Continuum states of the $3n$ system are studied with the response function for the transition from ^{3}H to $3n$ continuum state by an isospin excitation operator. One observes that the response function calculated with the AV18 nn potential does not reveal any resonance peak.

In view of the recent discrepancy in $3n$ calculations on the existence of a $3n$ resonance state, I have examined three methods to bring an attractive effect to make the $3n$ system bind for extrapolating the $3n$ energy: to enhance a component of the nn potential, to introduce a three-body force, and to add an external attractive trapping potential. The first two methods are consistent with the nonexistence of $3n$ resonance state. In the last case, the attractive effect unusually reduces the exterior barrier caused by the P-wave centrifugal potential, which makes the extrapolations using calculated $3n$ binding energies difficult. The reason for the unsuccessful extrapolation for the trapping method is due to the longer range trapping potential destroying the potential barrier. This defect occurs in general, and the trapping method should be used carefully in studies of resonance states of few- and many-body systems.

[1] C. R. Howell, Q. Chen, T. S. Carman, A. Hussein, W. R. Gibbs, B. F. Gibson *et al.*, Phys. Lett. B **444**, 252 (1998).

[2] J. P. Miller, J. A. Bistirlich, K. M. Crowe, S. S. Rosenblum, P. C. Rowe, F. T. Shively *et al.*, Nucl. Phys. A **343**, 347 (1980).

[3] F. M. Marqués, M. Labiche, N. A. Orr, J. C. Angélique, L. Axelsson, B. Benoit *et al.*, Phys. Rev. C **65**, 044006 (2002).

[4] K. Kisamori, S. Shimoura, H. Miya, S. Michimasa, S. Ota, M. Assie *et al.*, Phys. Rev. Lett. **116**, 052501 (2016).

[5] S. Gandolfi, H. W. Hammer, P. Klos, J. E. Lynn, and A. Schwenk, Phys. Rev. Lett. **118**, 232501 (2017).

[6] J. G. Li, N. Michel, B. S. Hu, W. Zuo, and F. R. Xu, Phys. Rev. C **100**, 054313 (2019).

[7] A. Hemmdan, W. Glöckle, and H. Kamada, Phys. Rev. C **66**, 054001 (2002).

[8] R. Lazauskas and J. Carbonell, Phys. Rev. C **71**, 044004 (2005).

[9] A. Deltuva, Phys. Lett. B **782**, 238 (2018).

[10] A. Deltuva, Phys. Rev. C **97**, 034001 (2018).

[11] A. Deltuva and R. Lazauskas, Phys. Rev. Lett. **123**, 069201 (2019).

[12] S. Gandolfi, H. W. Hammer, P. Klos, J. E. Lynn, and A. Schwenk, Phys. Rev. Lett. **123**, 069202 (2019).

[13] P. Truöl and J. P. Miller, arXiv:1708.04459.

[14] L. D. Faddeev, Zh. Eksp. Teor. Fiz. **39**, 1459 (1961) [Sov. Phys. JETP **12**, 1014 (1961)].

[15] M. Palarczyk *et al.*, Phys. Rev. C **58**, 645 (1998).

[16] T. Wakasa, E. Ihara, M. Dozono, K. Hatanaka, T. Imamura, M. Kato *et al.*, Phys. Rev. C **77**, 054611 (2008).

[17] S. Ishikawa, Prog. Theor. Exp. Phys. **2018**, 013D03 (2018).

[18] S. Ishikawa, Few-Body Syst. **32**, 229 (2003).

[19] S. Ishikawa, Phys. Rev. C **80**, 054002 (2009).

[20] S. Ishikawa, Phys. Rev. C **87**, 055804 (2013).

[21] R. B. Wiringa, V. G. J. Stoks, and R. Schiavilla, Phys. Rev. C **51**, 38 (1995).

[22] S. Ishikawa and M. R. Robilotta, Phys. Rev. C **76**, 014006 (2007).

[23] E. Hiyama, R. Lazauskas, J. Carbonell, and M. Kamimura, Phys. Rev. C **93**, 044004 (2016).

[24] E. Hiyama, B. F. Gibson, and M. Kamimura, Phys. Rev. C **70**, 031001(R) (2004).